Improved Transmission-Line Attenuators for Integrated Power Filters in the RF Band

Colin Kydd Campbell, *Life Fellow, IEEE*, Jacobus Daniel van Wyk, *Fellow, IEEE*, and Pieter Wolmarans

***Abstract*—Differential mode electromagnetic interference (EMI) at radio frequencies (RF) in compact integrated power electronic converter modules—as due in part to semiconductor switching and structural electromagnetic coupling—can be suppressed by the use of lossy transmission line lowpass filters. A previously reported lowpass filter design for such a system employed a $Cu-Al_2O_3-Ni-BaTiO_3-Ni-Al_2O_3-Cu$ lossy *uniform width* planar transmission line. where the low-permittivity Al_2O_3 ceramic wafer merely separates the Cu and Ni conductors. The higher-conductivity Cu conductors served to handle kW-level power frequencies. Above power frequencies, skin-depth restrictions cause current diversion from the Cu line into the inner segment of $Ni-BaTiO_3-Ni$ that provides subsequent attenuation of milliwatt-level spurious RF interference. Velocity reduction due to the high-permittivity barium titanate $(BaTiO_3)$ ceramic $(\varepsilon_r \sim 12,000)$ enabled compact integrated package size construction (e.g., 10 mm $\times$ 1.5 mm $\times$ 130 mm).**

With the aim of increasing the lowpass cutoff response slope, the current paper examines a prototype non-*uniform* (in width) planar $Ni-BaTiO_3-Ni$ constituent attenuator segment. For ease of one-dimensional (1-D) ABCD matrix analysis, a four-section $Ni-BaTiO_3-Ni$ planar attenuator—comprised of four cascaded uniform sections of decreasing step width—was fabricated as a first approximation to an exponential taper.

While good agreement was obtained between the predicted and experimental responses of the reverse-connected (narrow-to-wide) attenuator up to about 30 MHz, the discrepancy between the experimental and theoretical forward-connected (wide-to-narrow) frequency responses is attributed here to three-dimensional current constrictions at step interfaces. It is postulated that this can be overcome by the alternate use of a linearly- or an exponentially-tapered line.

***Index Terms*—Cu conductors, differential mode electromagnetic interference (EMI), exponentially-tapered line, linearly-tapered line, lowpass filter, planar attenuator, radio frequencies (RF), reverse-connected attenuator.**

I. Introduction

THE INTEGRATION of power-electronic converters into compact hybrid three-dimensional (3-D) packages or integrated power electronics modules (IPEMs) can lead to a significant increase in both power-density levels and electromagnetic coupling between components [1], [2]. Packaging designs catering for the former require a thorough knowledge of the thermal dissipation characteristics of the constituent components [3]. Such components can include; for example, planar integrated inductance–capacitance–transformer (LCT) modules, with dimensions in the order of 100 $\times$ 100 mm, as employed in high-frequency partial-resonant power converters operating at multikilowatt levels [4], [5]. For hybrid multikilowatt power-electronics converters this approach provides an alternative manufacturing technique, as well as reduces the converter volume significantly [5]. The increased electromagnetic coupling and associated reduction in volume/increase in power density leads to reduced electromagnetic compatibility (EMC) and higher levels of generation of electromagnetic interference (EMI). The reduced converter volume now furthermore requires a reduced volume and lower profile for the EMI filters. This requirement does not correspond to what can be achieved with the present technology of constructing these filters with discrete components. All these considerations lead to a paradigm shift in filter technology for compact, low profile high density integrated EMI filters.

The need for RF EMI suppression in electronic systems has been known for many years. Related techniques have involved the use of lowpass coaxial and other cables in military and aerospace applications (U.S. Specification MIL-C-85 485). These have included the use of absorptive lowpass cable filters for elimination or reduction of out-of-band interference [6], [7]. However, all of these prior RF filtering techniques involve structures that are too large for IPEM packaging.

Compact alternative RF lowpass transmission-line filter designs for IPEMs must satisfy three main design prerequisites. These are:

1) for compactness, the propagating e-m wave velocity must be reduced to a fraction of its free-space velocity value of 3×10^8 m/s;
2) the structure must be electrically and mechanically able to handle 1 kW to 10 kW at power frequencies with 300 to 500 V and 30 A current ratings, including dc;
3) the RF lowpass filter cutoff slope should be as large as possible (e.g., >40 dB/decade).

Applications of integrated RF lowpass filters include those for hybrid integrated power electronics converters with kW-level planar inductor–inductor–capacitor–transformer (L–L–C–T) structures, handling power densities in the order of 240 W/in^3 (14.6 W/cm^3) [8]. In these structures RF-EMI interference can be due to switching in the converter, enhanced by ringing due to structural inductance and capacitance in the devices and in the packaging. For other integrated converter types it has also been demonstrated that high levels of electromagnetic interference (EMI) due to high-speed turn-on and

Manuscript received June 1, 2002; revised October 31, 2003. This work was supported by the Engineering Research Center Program, National Science Foundation under National Science Foundation Award ECC-9731677. This work was recommended for publication by Associate Editor A. Deutsch upon evaluation of the reviewers' comments.

The authors are with the Center for Power Electronic Systems, Virginia Polytechnic Institute and State University, Blacksburg, VA 24061 USA (e-mail: daan@vt.edu).

Digital Object Identifier 10.1109/TCAPT.2004.828569

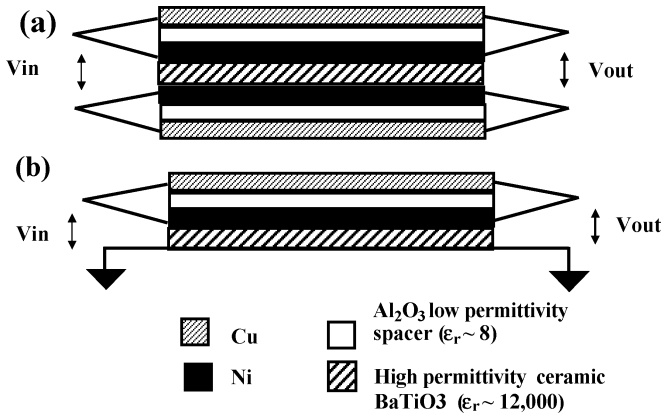

Fig. 1. Cross section (not to scale) of illustrative $\mathrm{Cu} - \mathrm{Al_2O_3} - \mathrm{Ni} - \mathrm{BaTiO_3} - \mathrm{Ni} - \mathrm{Al_2O_3} - \mathrm{Cu}$ lossy parallel-plate transmission line lowpass filter with constituent $\mathrm{Ni} - \mathrm{BaTiO_3} - \mathrm{Ni}$ attenuator segments. (a) With isolated input/output connections. (b) With common ground return.

turn-off transitions in associated semiconductor transistors and fast-recovery diodes can be significant up to 100 MHz [9].

This paper reports one proposed technique for enhancing the suppression of differential mode EMI (1 MHz to 100 MHz) over that in a previously reported compact ($10 \times 1.5 \times 130$ mm) low profile *uniform width*, lossy planar transmission line filter, with the layered copper–alumina–nickel–barium titanate–nickel–alumina copper ($\mathrm{Cu} - \mathrm{Al_2O_3} - \mathrm{Ni} - \mathrm{BaTiO_3} - \mathrm{Ni} - \mathrm{Al_2O_3} - \mathrm{Cu}$) structure shown in Fig. 1 [10], [11]. The modification examined here involves converting the structure to one of *nonuniform* width, as an extension of early work (1971) on low-frequency distributed RC filters using exponential tapers for enhanced cut-off slope [12], [13]. Since the RF attenuation is provided by the interior $\mathrm{Ni} - \mathrm{BaTiO_3} - \mathrm{Ni}$ layers of Fig. 1, attention here focussed solely on the response of this segment. As a first approximation to an exponential taper—while allowing for one-dimensional (1-D) ABCD lossy transmission-line analysis—the four-section $\mathrm{Ni} - \mathrm{BaTiO_3} - \mathrm{Ni}$ tapered attenuator segment of Fig. 2 was examined experimentally and theoretically.

While good agreement was obtained between the predicted and experimental responses of the reverse-connected (narrow-to-wide) attenuator up to about 30 MHz, the discrepancy between the experimental and theoretical forward-connected (wide-to-narrow) frequency responses is attributed here to 3-D current constrictions at step interfaces. It is postulated that this can be overcome by the alternate use of a linearly-tapered or an exponentially-tapered line.

II. Prior Techniques for Improving RF Attenuation

For attainment of small size with planar transmission lines, the wave velocity must be considerably reduced from its free-space value by using either a using high-permittivity low-loss dielectric ($\mathrm{v} = \mathrm{c}/\sqrt{\varepsilon_\mathrm{r}}$) or a high-permeability low-loss magnetic material ($v = c/\sqrt{\mu_\mathrm{r}}$) as the wave propagation medium. The use of very high-permittivity (e.g., $\varepsilon_\mathrm{r} \sim 12{,}000$) $\mathrm{BaTiO_3}$ ceramic wafers has been reported for these integrated filter designs, using a planar *uniform* module with the cross section and composition of Fig. 1. Package dimensions were width $w =$ 10 mm, thickness $t = 1.5$ mm, and length $l = 130$ mm [11]. Another prior technique employed a high-permeability core of cobalt-based amorphous ribbons ($\mu_\mathrm{r} = 450$), with thickness of 15 μm and width of 10 μm in a meander-line structure [9].

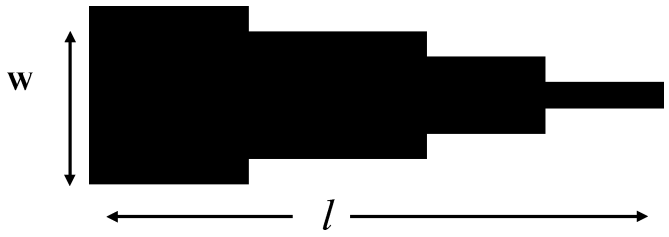

Fig. 2. Plan view of four-section forward-tapered $\mathrm{Ni} - \mathrm{BaTiO_3} - \mathrm{Ni}$ attenuator segment (Not to scale).

For filtering of very-high frequency transmissions, it is also known that use of a *nonuniform* (in width or in composition) microwave transmission line can improve its bandpass roll-off characteristics, as compared with a uniform one. [14]. This technique has also been applied to increasing the low frequency cut-off slope of distributed Resistance–Capacitance (RC) filters for integrated circuit applications. For such distributed low frequency RC filters (where inductance parameters may be neglected) it has been demonstrated that an increase in lowpass cut-off slope could be achieved by the use of exponentially (or other) tapered (in width) geometry [12], [13].

A previously reported compact IPEM RF lowpass filter [11] consisted of a planar uniform lossy transmission line composite with the $\mathrm{Cu} - \mathrm{Al_2O_3} - \mathrm{Ni} - \mathrm{BaTiO_3} - \mathrm{Ni} - \mathrm{Al_2O_3} - \mathrm{Cu}$ cross-section of Fig. 1, for RF suppression in the range 1 to 100 MHz. The copper layers are designed to carry multikilowatt-level power-frequency transmissions with negligible loss. The higher-conductivity ($\sigma_\mathrm{Cu} = 5.8 \times 10^7\ \mathrm{S/m}$) Cu layer thickness is dimensioned such that impedance increase for frequencies appreciably higher than the power frequencies will divert current into the lower-conductivity ($\sigma_\mathrm{Ni} = 1.45 \times 10^7\ \mathrm{S/m}$) Ni conductor. In turn, subsequent skin-depth constriction by the Ni conductor at RF frequencies will, (in conjunction with the $\mathrm{BaTiO_3}$ shunt capacitance), dictate the RF 3-dB cut-off frequency and subsequent attenuation roll-off response.

Motivation for this approach came from early (1971) experiments on the use of exponential tapers to enhance the lowpass cut-off slope of low-frequency distributed RC filters for integrated circuits [14]. To this end, a prototype four-section attenuator with the planar geometry of Fig. 2 was fabricated, where uniform segments of differing width were employed, as a first approximation to an exponential taper. This permitted cascaded 1-D ABCD matrices to be applied to a lossy (R-L-C-G) transmission-line analysis, as outlined below. For ease of analysis, proximity effects on the current distribution, fringing fields and 3-D current crowding at sharp conductor changes were neglected.

III. Lossy Planar Transmission Lines

A. ABCD Matrix Computations

Cascaded 1-D ABCD matrix computations [15] were employed to obtain the frequency response of the four-section lossy $\mathrm{Ni} - \mathrm{BaTiO_3} - \mathrm{Ni}$ attenuator segment of Fig. 2, with frequency-

dependent distributed R-L-C-G parameters taken as per unit length (m^{-1}). Here, $R(f)$ is the Ni conductor series resistance as modified by skin-depth penetration, $L(f)$ = conductor total internal and external series inductance as also modified by skin-depth penetration, C = distributed shunt capacitance of the high-permittivity ($\varepsilon_{\mathrm{r}} \sim 12,000$ at 1 MHz) $\mathrm{BaTiO_3}$ ceramic, with dissipation factor $tan\Delta = G/\omega C$, where $G = G(f)$ = distributed shunt leakage conductance.

The series impedance $Z = Z(f)$ and shunt admittance $Y = Y(f)$ per unit length for individual attenuator segments are given by

$$Z = Z(f) = (R(f) + j\omega L(f)) \quad (\Omega/\mathrm{m}) \tag{1a}$$

$$Y = Y(f) = (G(f) + j\omega C(f)) \quad (\mathrm{S/m}) \tag{1b}$$

while the characteristic impedance $Z_{\mathrm{o}} = Z_{\mathrm{o}}(f)$ and propagation constant $\gamma = \gamma(f)$ for these become

$$Z_o = \sqrt{\frac{Z(f)}{Y(f)}} \quad (\Omega) \tag{2a}$$

$$\gamma = \alpha + j\beta = \sqrt{Z(f)Y(f)} \quad (\mathrm{m}^{-1}). \tag{2b}$$

In this planar design, the series impedance Z and shunt admittance Y will effect lowpass filter action at a frequency largely dictated by the skin-depth constriction in the Ni conductor.

B. Approximation for Parallel Plane Transmission Line

1) Distributed Series Resistance $R(f)$: We consider a two conductor transmission line with plane parallel lines of width w, whose thickness t becomes comparable to its skin depth δ at RF frequencies in the range of interest for the lowpass filter. For the structure of Fig. 1(a) the distributed resistance $R(f)$ per unit length is approximated as

$$\begin{array}{l} R(f) = \frac{2\rho}{wt} \; for \; \delta > t \\ R(f) = \frac{2\rho}{w\delta} \; for \; \delta < t \end{array} \quad (\Omega/\mathrm{m}) \tag{3}$$

where the factor 2 is applicable if the isolated two-conductor connection of Fig. 1(a) is employed; with factor 1 employed for Fig. 1(b).

2) Distributed Series Inductance $L(f)$: In this design we assume that the conductor widths w are much greater than the spacing d between them. The field pattern in the inter-conductor space is then approximated as that for infinite planes [15], so that the *internal* inductance $L_{\mathrm{int}}(f)$ per unit length is given by

$$\begin{array}{ll} L_{\mathrm{int}}(f) \approx \frac{2}{3}\mu_o\mu_r\frac{t}{w} & \delta > t \\ L_{\mathrm{int}}(f) \approx \frac{2}{3}\mu_o\mu_r\frac{\delta}{w} & \delta < t \end{array} \quad (\mathrm{henry/m}) \tag{4}$$

where the additional factor of 2 again applies to the isolated structure of Fig. 1(a). Additionally, the distributed external inductance $L_{\mathrm{ext}}(f)$ per unit length is approximated as [16]

$$L_{ext}(f) \approx \mu_o\frac{d}{w} \tag{5}$$

where μ_{r} = nickel relative permeability, and $\mu_{\mathrm{o}} = 4\pi \times 10^{-7}$ henry/m = permeability of free space, giving the approximate combined inductance $L(f) \approx L_{\mathrm{int}}(f) + L_{\mathrm{ext}}(f)$ (henry/m).

3) Distributed Capacitance $C(f)$: For width $w \gg d$, we neglect fringing effects and approximate the distributed capacitance $C(f)$ as

$$C(f) \approx \varepsilon_r\varepsilon_o\frac{w}{d} \quad (\mathrm{F/m}) \tag{6}$$

where $\varepsilon_{\mathrm{r}} = \mathrm{BaTiO_3}$ relative permittivity, and $\varepsilon_{\mathrm{o}} = 8.85 \times 10^{-12}$ F/m = permittivity of free space.

4) Distributed Conductance $G(f)$: Again neglecting fringing effects, we approximate the distributed shunt of the $\mathrm{BaTiO_3}$ ceramic dielectric as

$$G(f) \approx \omega C(f) tan\Delta \quad (\mathrm{S/m}) \tag{7}$$

where $tan\Delta$ = frequency-dependent dissipation factor [16]. For high-permittivity ferroelectric ceramics such as $\mathrm{BaTiO_3}$, both $C(f)$ and $tan\Delta$ can be functions of frequency and voltage, depending on the pre-sintering composition and after-sintering structure of the ceramic dielectric. In filter construction, these will dictate whether grain-dipole orientations or Debye polar relaxation at the grain-boundary interfaces dominate the $C-V$ response [17].

5) Frequency Response: From the above, the voltage and current response functions may be obtained by ABCD matrix and two-port representation, so that

$$\begin{bmatrix} V_{in} \\ I_{in} \end{bmatrix} = \begin{bmatrix} A & B \\ C & D \end{bmatrix} \begin{bmatrix} V_{out} \\ I_{out} \end{bmatrix} \tag{8a}$$

where, for the four-section structure of Fig. 2

$$\begin{bmatrix} A & B \\ C & D \end{bmatrix} = \begin{bmatrix} A1 & B1 \\ C1 & D1 \end{bmatrix} \begin{bmatrix} A2 & B2 \\ C2 & D2 \end{bmatrix} \begin{bmatrix} A3 & B3 \\ C3 & D3 \end{bmatrix} \begin{bmatrix} A4 & B4 \\ C4 & D4 \end{bmatrix} \tag{8b}$$

and individual matrices have the hyperbolic function form

$$\begin{bmatrix} A* & B^* \\ C^* & D^* \end{bmatrix} = \begin{bmatrix} cosh(\gamma l)^* & Z_o^* sinh(\gamma l)^* \\ \frac{1}{Z_o^*} sinh(\gamma l)^* & cosh(\gamma l)^* \end{bmatrix} \tag{8c}$$

for individual propagation constants γ^*, lengths l^*, and characteristic impedances Z_{o}^*, so that

$$\frac{V_{out}}{V_{in}} = \frac{1}{A + \left(\frac{B}{R_L}\right)} \tag{9}$$

where R_{L} = load resistance.

IV. Fabrication Highlights

The EMI filters under study here were fabricated by one of the authors (PW). Highlights of their construction details are given below.

A. $\mathrm{BaTiO_3}$ Wafer Tile Preparation

Commercial high-permittivity ($\varepsilon_{\mathrm{r}} \sim 12,000$) $\mathrm{BaTiO_3}$ wafer tiles were employed here. To the authors' knowledge, only one company (in Italy) currently manufactures such high-permittivity $\mathrm{BaTiO_3}$ ceramic wafers. Data on their exact fabrication preparation method, as well as their doping and/or impurity contents, were not available to the authors. However, from previous experiments on $\mathrm{BaTiO_3}$ ceramic fabrication conducted by two of the authors (CKC, JDvW) it was observed that its maximum permittivity value as well as its voltage and frequency-dependent permittivity, can be significantly controlled by selective dopant addition to the powder prior to the sintering process,

as well as by subsequent internal strain developed during the sintering process itself [17], [18]. The ceramic wafer tiles used here were of width 6 cm and length 12 cm, with a thickness of only 150 μm. These required considerable care in handling and packaging, due to their brittle state as attributed by us to internal strains.

Prior to the EMI filter fabrication in our laboratory, the ceramic wafer tiles were washed in acidic and base solutions, followed by rinsing with deionized water in an ultrasonic bath. Next, they were suspended above a hotplate set at 40 °C to drive off moisture. The dry tiles were then further cleaned in an argon gas plasma.

B. Nickel Metallization

The Ni metallization of these ceramic wafer tiles was conducted in a three-stage process. The first stage involved deposition of a seed layer of titanium (Ti), to promote adhesion between the ceramic surface and the ensuing Ni seed-layer deposition. This was carried our in a high-vacuum system employing a glow discharge sputter deposition process with a Ti target disk of 99.95%+ purity.

The second deposition stage was also conducted in a high-vacuum system, this time involving the glow discharge sputter deposition of an overlying seed layer of Ni from a similarly pure target disk. Both sides of the wafer tiles were seeded in this manner. (Note that, due to its minimal thickness, the ceramic wafer tile could not be metalized only on one side, as this would result in curvature degradations formed by metal/ceramic surface stresses).

Once both sides had been Ni seed-sputtered in high vacuum, the third step was to deposit a Ni conductor layer in an electroplating solution—where the nickel was deposited simultaneously on to both sides to cover the entire tile.

C. Transmission Line Conductors

Standard photolithographic techniques were used to form the Ni conductor transmission line conductors, while removing undesired regions of Ni and Ti. The undesired nickel was removed with heated ferric-chloride in a spray etcher. The undesired Ti was removed with tetrafluoromethane (TFT). After etching, the mask was removed and the tile chemically cleaned and checked for any obvious visible structural defects.

D. Alumina Separation Layer

Thin low-permittivity alumina $(\mathrm{Al_2O_3})$ $(\varepsilon_\mathrm{r} \sim 4.5 - 8.4)$ substrates of 0.5 mm thickness were employed to separate the inside (Ni) and outside (Cu) conductors, while also providing structural rigidity. The outer side of the $\mathrm{Al_2O_3}$ was first partially metalized—this time with seed layers of Ti and Cu, using the plasma vacuum deposition. This was followed by the final Cu deposition and conductor pattern etching. End terminals were attached, and the filter was sealed with a plastic encapsulant. Finally, and as a partial check on its integrity against flaws, the composite filter structure was subjected to a 150 °C thermal cycle while measuring its capacitance at a dc voltage of 600 V.

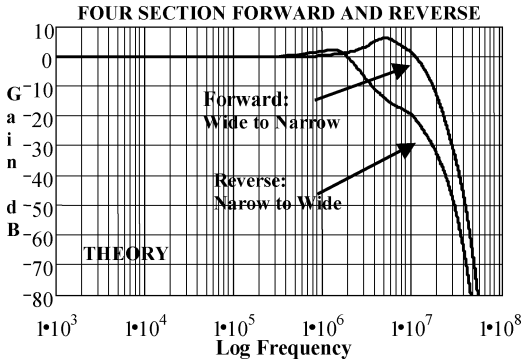

Fig. 3. ABCD lossy transmission line analysis of forward and reverse cut-off frequency responses of four-section planar Ni attenuator section of Fig. 2. Horizontal scale: 1 kHz to 100 MHz. Vertical scale: +10 to −80 dB.

V. Case Study of Four-Section Tapered Line

A. Device Parameters and Instrumentation

The four-section inline $\mathrm{Ni} - \mathrm{BaTiO_3} - \mathrm{Ni}$ attenuator of Fig. 2 was fabricated on a single $\mathrm{BaTiO_3}$ ceramic wafer ($w =$ 60 mm, $l = 130$ mm, $t = 150$ μm, $\varepsilon_\mathrm{r} \sim 12{,}000$). Nickel widths plated on this were successively 40 mm, 20 mm, 10 mm, and 5 mm, with the length of each section set at 25 mm. The nickel strip thickness throughout was 17 μm, with relative permeability taken as $\mu_\mathrm{r} \sim 100$ and conductivity $\sigma = 1.45 \times 10^7$ S/m. As well, the dissipation factor for the $\mathrm{BaTiO_3}$ ceramic was approximated as $tan\Delta = 0.0035\sqrt{(f/10^6)}$ over the range 1 kHz to 100 MHz.

Fig. 3 shows the predicted forward (wide-to-narrow) and backward (narrow-to-wide) magnitude responses over the range 1 kHz to 100 MHz, where the lowpass roll-off at ∼1 MHz is attributed to Ni skin-depth constriction, and "peaks" in the responses around cutoff are due to inductance effects. Note that parameters were calculated for the common-ground configuration of Fig. 1(b), to conform with subsequent measurements on a common-ground gain-phase analyzer.

The filter frequency response was measured with an HP 4194A Gain-Phase Analyzer, with common input-output ground, over the frequency range 1 kHz to 100 MHz. Prior to measurements, the analyzer was calibrated for 0 dB reference using a straight-through input/output connection. The noise floor was below 100 dB with the filter disconnected.

B. Forward and Reverse Measurements

Fig. 4 shows the experimental forward (wide-to-narrow) and backward (narrow-to-wide) magnitude responses of the four-section attenuator of Fig. 2 The experimental frequency response of the reverse-connected (narrow-to-wide) filter was in good agreement up to about 30 MHz with the predicted one shown in Fig. 3, both in terms of its slope and cut-off values. Moreover, if the filter is modeled at cut-off as a cascade connection of R-L-C resonator and quarter-wave transformers, its cut-off frequency f_co can approximated as $f_\mathrm{co} = \{\mathrm{c}/\sqrt{\varepsilon_\mathrm{r}})/(4 \times 25 \times 10^{-3}) \approx 27.3$ MHz, which is in reasonable agreement with the responses shown in Fig. 3 and Fig. 4.

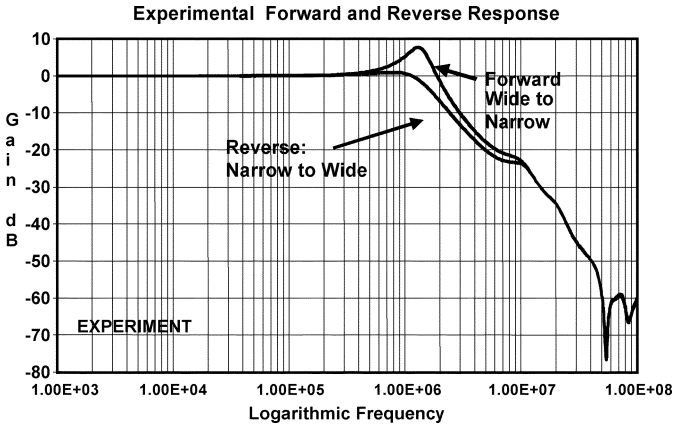

Fig. 4. Experimental frequency responses for four-section forward-connected and reverse-connected $\mathrm{Ni-BaTiO_3-Ni}$ line with 50 Ω load on HP gain-phase analyzer. Horizontal scale: 1 kHz to 100 MHz. Vertical scale: $+10$ to -80 dB.

There is disagreement, however, between the predicted and experimental frequency responses of the forward-connected (wide-to-narrow) lowpass filter, in both its 3-dB roll-off frequency and roll-off slope. The experimental 3-dB roll off point was about 10 MHz less than predicted in Fig. 3. Experimentally, the initial 3-dB cut off slope of the forward connected attenuator is $\sim$50 dB/decade over about the first octave, as compared with $\sim$40 dB/decade in the uniform-width structure of [11]. Possible explanations for these discrepancies, as well as a suggested remedy are as given in the following section. Overall, however, the test attenuator studied here serves to demonstrate that the cut-off response can indeed be modified by shaping the width of the structure, as previously evidenced in nonuniform distributed RC lowpass filters [13].

VI. Discussion

The RF lowpass roll-off characteristics have been examined for a prototype nonuniform (in width) $\mathrm{Ni-BaTiO_3-Ni}$ attenuator for a $\mathrm{Cu-Al_2O_3-Ni-BaTiO_3-Ni-Al_2O_3-Cu}$ RF-EMI filter.

As noted above, good agreement is obtained between the predicted and experimental responses of the reverse-connected attenuator up to about 30 MHz, thus serving to validate—at least in part—the concepts and analytical method employed here

In considering the discrepancy between the experimental and theoretical forward-connected filter frequency responses, it is postulated here that this can be attributed principally to 3-D current crowding at skin-depth frequencies, that could affect both the inductance and conductance in these regions. This could be manifest as an effective reduction in the step size at each junction, with a commensurate change in the 3-dB cut off frequency and roll-off slope. This postulate was subsequently checked, and supported, by observing the roll-off characteristics of a *uniform* Ni test attenuator. A proposed solution for enhancing the roll-off response characteristic of the forward-connected structure would be either to use

a) a longer structure with more steps and smaller step sizes;
b) a linearly-tapered structure;
c) an exponentially-tapered structure.

Overall filter frequency response performance will also be dictated in part by the permeability of the Ni attenuator itself. This can vary considerably, depending on the processing technique [16]. Published permeability values quoted for Ni are routinely given only for the *real part* of the complex permeability, and these can range from 50 [19] to 600 [20]. Moreover, no information was available to the authors on the *complex* permeability component of Ni over the frequency range employed here.

Furthermore, it is realized that if the current in the outer copper busbars (Fig. 1) has an appreciable dc component, the effective permeability of the Ni layers in the attenuator will be affected. This could lead to a detrimental change in the frequency response of the filter, depending on the values of the permeability in our manufactured layers, as well as the sensitivity of the overall damping on the Ni permeability. Studies are at present in progress to isolate these effects. However, even if it is established that the effect on the frequency response is detrimental, filters using Ni metallization will still be applicable in the output busbars of power electronic dc–ac converters, where dc components are absent.

References

[1] J. A. Ferreira and J. D. van Wyk, "Electromagnetic energy propagation in power electronic converters," *Proc. IEEE*, vol. 89, pp. 876–889, June 2001.
[2] J. D. van Wyk and F. C. Lee, "Power electronics technology at the dawn of the new millennium," in *Proc. 30th IEEE Annual Power Electronics Specialists Conf. (PESC)*, vol. 1, June 1999, pp. 3–10.
[3] S.-Y. Lee, L. Zhao, J. T. Strydom, W. G. Odendaal, and J. D. van Wyk, "Thermal analysis for a series LC-integrated passive resonant module based on finite element modeling," in *Proc. 33rd IEEE Annual Power Electronics Specialists Conf. (PESC)*, vol. 2, June 2002, pp. 1009–1014.
[4] P. A. Janse van Rensburg, J. D. van Wyk, and J. A. Ferreira, "Design and construction of a generic multi-kVA planar integrated LCT for a family of series resonant converters," in *Proc. 31st IAS Annual IEEE Industry Applications Society Meeting*, vol. 3, Oct. 6–10, 1996, pp. 1361–1368.
[5] J. D. van Wyk and J. A. Ferreira, "Evaluation and future prospects of an integration technology for hybrid multikilowatt power electronic converters," in *Proc. 7th European Conf. Power Electronics and Applications (EPE'97)*, vol. 1, Sept. 1997, pp. 1.194–1.199.
[6] F. Mayer, "Absorptive low-pass cables: state of the art and an outlook to the future," *IEEE Trans. Electromagn. Compat.*, vol. EMC-28, pp. 7–17, Feb. 1986.
[7] H. W. Denny and W. B. Warren Jr., "Lossy transmission line filters," *IEEE Trans. Electromagn. Compat.*, vol. EMC-10, pp. 363–371, Dec. 1968.
[8] R. Chen, B. Yang, F. Canales, and J. D. van Wyk, "Volumetric optimal design of passive integrated power electronic module for distributed power system front-end DC/DC converter," in *Proc. IEEE Annual Industry Applications Conf.*, vol. 3, Oct. 2002, pp. 1758–1765.
[9] T. Sato, S. Ikeda, K. Yamasawa, and T. Mizoguchi, "Transmission line low-pass filter for switching power supplies," in *Proc. 29th Annual IEEE Power Electronics Specialists Conf. (PESC'98)*, vol. 2, 1998, pp. 1972–1978.
[10] J. D. van Wyk Jr, A. Cronje, J. D. van Wyk, and C. K. Campbell, "Integrated power filters utilizing skin-and proximity effects based low pass interconnects," in *Proc. VDE/IEEE 2nd Int. Conf. Integrated Power Systems (CIPS)*, Bremen, Germany, June 2002, pp. 73–82.
[11] P. J. Wolmarans, J. D. van Wyk Jr, J. D. van Wyk, and C. K. Campbell, "Technology for integrated RF-EMI transmission line filters for integrated power electronics modules," in *Proc. IEEE Annual Industry Applications Conf.*, vol. 3, Oct 2002, pp. 1774–1780.
[12] M. Ghausi and J. J. Kelly, *Introduction to Distributed Parameter Networks With Applications to Integrated Circuits*. New York: Holt, Rinehart and Winston, 1968.

[13] J. A. Carson, C. K. Campbell, P. L. Swart, and F. J. Vallo, "Effect of dielectric losses on the performance of evaporated thin-film distributed RC notch filters," *IEEE J. Solid-State Circuits*, vol. SC-6, pp. 120–124, June 1971.
[14] R. W. Klopfenstein, "A transmission line taper of improved design," in *Proc. IRE'56 Conf.*, vol. 44, Jan. 1956, pp. 31–35.
[15] R. G. Brown, R. A. Sharpe, W. L. Hughes, and R. E. Post, *Lines, Waves, and Antennas*, 2nd ed. New York: Ronald Press, 1973.
[16] R. A. Chipman, "Theory and problems of transmission lines," in *Schaum's Outline Series*. New York: McGraw-Hill, 1968.
[17] C. K. Campbell, J. D. van Wyk, and M. F. K. Holm, "Improving the frequency response of ceramic dielectrics for high power applications in power electronic converters," *IEEE Trans. Comp., Packag., Manufact. Technol. A*, vol. 19, pp. 508–515, Dec. 1996.
[18] C. K. Campbell, J. D. vanwyk, and M. F. K. Holm, "Development of large-area ceramics with optimized depletion regions as dielectrics for planar power electronics," *IEEE Trans. Comp., Packag., Manufact. Technol. A*, vol. 21, pp. 492–499, Sept. 1998.
[19] H. W. Sams and Co., "Reference Data for Radio Engineers," Tech. Rep., 1972.
[20] J. D. Kraus, *Electromagnetics*, 3rd ed. New York: McGraw-Hill, 1984, p. 216.

Colin K. Campbell (M'56–SM'67–F'86–LF'93) was born in Scotland in 1927. He received the B.Sc. degree (with honors) in electrical engineering and the Ph.D. degree in low-temperature physics from St. Andrews University, Scotland, in 1952 and 1960, respectively, the D.Sc. degree in engineering and applied science from the University of Dundee, Scotland, in 1984, and the S.M. degree in electrical engineering from the Massachusetts Institute of Technology, Cambridge, in 1953.

During World War II, he first trained as a Radio Operator for the British Merchant Navy, followed by service in the Royal Corps of Signals, British Army. From 1946 to 1948, he was a Communications Engineer with the Foreign Office, London, the British Embassy, Washington, D.C., and the British Delegation to United Nations, New York. He has also served in the military forces of Canada, and from 1962 to 1968 was Commanding Officer of 201 University Squadron, Royal Canadian Air Force Primary Reserve. He is the author of 1989 and 1998 textbooks on SAW devices and SAW signal processing. He was with McMaster University, Hamilton, ON, Canada, from 1960 to 1989, where he was a Professor of electrical and computer engineering, and is now an Emeritus Professor.

Dr. Campbell received "The Inventor" insignia from Canadian Patents and Development, Ltd., the Eadie Medal of the Royal Society of Canada, in 1983, and the IEEE Best Paper Award in 2002. He is a Fellow of the Royal Society of Canada, a Fellow of the Engineering Institute of Canada, a Fellow of the Royal Society of Arts (London), a Member of the Electromagnetics Academy, and a Member of Sigma Xi.

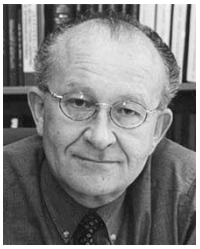

Jacobus Daniel van Wyk (F'90) received the M.Sc.Eng. degree from the University of Pretoria, South Africa, in 1966, the Dr.Sc.Tech. degree from the University of Technology, Eindhoven, The Netherlands, in 1969, and the D.Sc. degree (with high honors) in engineering from the University of Natal, South Africa, in 1996.

He has worked with the S.A. Iron and Steel Corporation, the University of Pretoria, and the Technical and Scientific Staff of the University of Eindhoven, The Netherlands, from 1961 to 1971. From 1971 to 1995, he was a Chaired Professor of Electrical and Electronic Engineering at Rand Afrikaans University, Johannesburg, South Africa, holding Chairs in Electronics and in Power Electronics until 1992. He founded the Industrial Electronics Technology Research Group, Faculty of Engineering, in 1978 and directed this unit until 1999. Since July 1995, he has held a special University Council Research Chair in Industrial Electronics at the Rand Afrikaans University. He joined the Bradley Department of Electrical and Computer Engineering, Virginia Polytechnic Institute and State University, Blacksburg, in January 2000, where he is the J. Byron Maupin Professor of Engineering, working in the National Science Foundation Engineering Research Center for Power Electronics Systems.

Dr. van Wyk received 20 prize paper awards, including more than 10 IEEE prize paper awards for some of this work, the prestigious IEEE William E. Newell Power Electronics Award in 1995, the IEEE Third Millennium Medal in 2000, and has received a range of other awards from IEEE Societies as well as from the South African Institute of Electrical Engineers. He is a Fellow of the South African Institute of Electrical Engineers and is active in several capacities within the IEEE and its Societies.

Pieter Wolmarans was born in South Africa. He received the B.Ing. and M.Ing. degrees from Rand Afrikaans University, Praetoria, South Africa, in 2000 and 2003, respectively.

From May 2001 until September 2002, he was with the Center for Power Electronics Systems, Virginia Polytechnic Institute and State University, Blacksburg, VA, as a Visiting Scholar in the High Density Integration Thrust, working on a project in connection with transmission line RF EMI filters. He is presently with the South African Team, SANAE, Antarctica, as an Electronics Specialist.